Available online at www.sciencedirect.com

ScienceDirect

www.elsevier.com/locate/jes

JES

JOURNAL OF
ENVIRONMENTAL
SCIENCES

www.jesc.ac.cn

Selective sorptive removal of Methyl Red from individual and binary component solutions by mesoporous organosilicas of MCM-41 type

Nadiia V. Roik*, Lyudmila A. Belyakova, Marina O. Dziazko

Chuiko Institute of Surface Chemistry of NAS of Ukraine, 17 General Naumov Str., Kyiv 03164, Ukraine

ARTICLE INFO

ABSTRACT

Organosilicas with chemically immobilized 3-aminopropyl and Methyl Red-containing surface groups were prepared by sol-gel condensation of tetraethyl orthosilicate and (3-aminopropyl)triethoxysilane in the presence of dye as part of the mixed micelles or dye-containing silane as silica source. The hexagonally arranged mesoporous structure of synthesized materials was confirmed by low-temperature nitrogen adsorption-desorption, x-ray diffraction, and TEM studies. Chemical composition of MCM-41-type organosilicas was established by FT-IR spectroscopy and chemical analysis of surface layer. Sorption of Methyl Red by organosilicas was studied from diluted phosphate buffer solutions in dependence of medium pH, duration of contact, and equilibrium concentration of dye. It was found that effective removal of Methyl Red takes place at pH values within a range of 2.5−5. Kinetic curves of Methyl Red sorption on organosilicas were analyzed by the Lagergren, Ho-McKey, and Weber-Morris kinetic models. It was found that the pseudo-second-order model fits the kinetics of Methyl Red sorption on all synthesized materials and the intraparticle diffusion is not the only one mechanism controlling the rate of Methyl Red sorptive removal. The parameters of equilibrium sorption of Methyl Red on organosilicas of MCM-41 type were calculated using Langmuir, Freundlich, Redlich-Peterson, and Brunauer-Emmett-Teller models. Sorption of acid dyes with geometry similar or substantially different from Methyl Red on mesoporous silicas was studied from single and binary component mixtures in aqueous solutions with pH 4.8 and 5.5. It was found that selective sorption process is highly dependent on the structural characteristics and protolytic state of silica surface as well as acid dye.

© 2020 The Research Center for Eco-Environmental Sciences, Chinese Academy of Sciences. Published by Elsevier B.V.

Introduction

Nowadays organic dyes are used in many fields of industry such as food, textile, printing, leather, paper, pharmaceutical, rubber, plastics, and cosmetics (Freeman and Peter, 2000; Klaus, 2003). As a consequence, huge amount of pollutants is released to surface water without suitable treatment. Among them azo dyes belong to the most numerous (60%−70% of all dyes) and hazardous class of pollutants. Potential danger for human arises from toxic, carcinogenic, mutagenic, and teratogenic effects of azo dyes and their biotransformation products (Ratna and Padhi, 2012; Zaharia and Suteu, 2012), aromatic amines. The significant attempts of scientists were focused on preventing human illnesses caused by azo dyes by development of affordable, effective, and simple techniques for their removal from wastewater. Promising results were achieved at wastewater purification by chemical (neutralization, electrolysis, reduction, oxidation, ion-exchange, photodegradation) and physical (flocculation, flotation, sedimentation, coagulation, sorption) treatment methods as well as by biodegradation (Shah, 2018; Singh and Arora, 2011; Singh and Singh, 2017; Vital

---

* Corresponding author.
E-mail: roik_nadya@ukr.net (N.V. Roik).

et al., 2016). However, because of more stringent effluent treatment regulations, it is important to develop techniques and approaches providing complete removal of harmful azo dye pollutants.

Sorption is one of the most widely used and promising methods of wastewater purification in terms of cost, simplicity of realization, and efficiency. Various materials were used for sorptive removal of dyes from aqueous solutions, including polymers, activated carbon, guargam powder, agricultural waste, silica, etc (Abbas, 2013; Alaguprathana and Poonkothai, 2017; Buvaneswari and Kannan, 2010; Enenebeaku et al., 2017; Foo and Hameed, 2010; Ghemati and Aliouche, 2014; Krysztafkiewicz et al., 2002; Panic et al., 2013; Santhi et al., 2010; Saxena and Sharma, 2016; Wu et al., 2014). Practical application of sorption may be limited by problems related with regeneration, chemical stability, and low removal efficiency of used sorbents.

Over the past several decades silica materials with arranged mesoporous structure have attracted interest of scientists as dyes sorbents due to their outstanding properties of high surface area, tunable pore morphology, high sorption capacity, thermal and mechanical stability, and easy functionalization. Many researches examined sorption potential of silica materials with ordered mesoporous structure towards dye pollutants from aqueous solutions and revealed that it strongly depends on dye nature, structural characteristics of sorbent, and conditions of experiment (Anbia and Hariri, 2010; Juang et al., 2006; Lee et al., 2007; Mirzajani et al., 2016; Wu et al., 2012). As-synthesized silica materials may be good sorbents for the removal of basic dyes from wastewaters, whereas their effectiveness in sorption of acid ones is less pronounced (Anbia and Hariri, 2010; Juang et al., 2006; Lee et al., 2007; Mirzajani et al., 2016; Wu et al., 2012).

Sorption efficiency may be improved by physical or chemical modification of silica surface with suitable functional groups. Functionalized silica with ordered mesoporous structure was prepared by impregnation with poly(diallyldimethylammonium chloride) and its sorption properties were examined using nine different dyes with positive, neutral, and negative charges (Joo et al., 2009). Relatively large surface area and pore diameters in the mesopore range in combination with physical modification of surface layer results in high sorption performance of synthesized material in comparison with sorption ability of commercial silica Davisil possessing irregular pore structure and wide pore size distribution, and granular activated carbon impregnated with polyelectrolyte (Joo et al., 2009). Adsorptive modification of MCM-41 with sodium dodecyl sulfate realized by authors (Zanjanchi et al., 2011) results in creation of effective sorbent for cationic dye removal from aqueous solutions. The effect of surfactant template, ethyltrimethylammonium bromide, located in the pores of SBA-3 on the removal of dyes from aqueous solutions was studied in the work (Anbia et al., 2010). The attempt to achieve high sorption ability and hydrothermal stability of mesoporous materials was realized by authors (Boukoussa et al., 2017), which used Al-MCM-41 with physically adsorbed cationic surfactant and calcined Al-MCM-41 to remove Yellow dye from aqueous solutions.

Chemical modification is very helpful in the improvement of sorption characteristics of silica because of reliable retention of surface functional groups responsible for the specific interactions with adsorbate. The literature reports introduction of different functional groups in surface layer of silicas with ordered mesoporous structure to enhance theirs sorption affinity to dye molecules (Abkenar, 2018; Anbia and Salehi, 2012; Ho et al., 2003; Kang et al., 2016; Lewandowski et al., 2014; Santos et al., 2013; Zubieta et al., 2008). Chitosan treated silica with lamellar mesoporous structure was prepared to improve sorption ability towards both anionic (Tectilon Blue) and cationic (Rhodamine B) dyes used in the textile industry (Zubieta et al., 2008). Sorption efficiency

of ordered mesoporous silica SBA-3 towards acid dyes Acid Blue 113, Acid Red 114, Acid Green 28, Acid Yellow 127, and Acid Orange 67 was improved by chemical modification with amino-containing groups (3-aminopropyl, ethylenediamine, pentaethylene hexamine) (Anbia and Salehi, 2012). MCM-41 silica with grafted 3-aminopropyl groups exhibits relatively high adsorption capacity and efficiency in sorption of acid dyes Remazol Red (Santos et al., 2013) and Acid Blue 25 (Kang et al., 2016) due to the strong electrostatic interactions. At the same time, removal of basic dye Methylene Blue by silica with surface amino groups decreases in comparison with parent MCM-41 (Kang et al., 2016). Comparative study of sorptive removal of Acid Blue 25 and Methylene Blue dyes from wastewater was carried out on mesoporous silicas of MCM-41 type with grafted amino- and carboxylic functional groups (Ho et al., 2003). It was found that amino-containing adsorbent has a large sorption capacity and a strong affinity for the Acid Blue 25, whereas, material with surface carboxylic groups demonstrates excellent sorption capacity and selectivity for the Methylene Blue. The effective removal of Acid Brown 214 from aqueous solutions was achieved by use of fluorene functionalized SBA-15 (Abkenar, 2018). Functional groups with different charge were introduced by post-synthetic modification of MCM-41 with 1-methyl-3-(3-(trimethoxysilyl)propyl)-1H-imidazol-3-ium (positively charged), N-(3-(triethoxysilyl)propyl)gluconamide (neutral), and N-(3-(trimethoxysilyl)-propyl)ethylenediamine triacetic acid trisodium salt (negatively charged) (Lewandowski et al., 2014). In accordance with the sorption studies of Sunset Yellow FCF, Chromotrope 2R, and Alcian Blue-tetrakis(methylpyridinium) chloride, the most efficient removal of azo dyes proceeds on positively charged organosilica surface.

Due to the planar aromatic structure molecules of azo dyes are easily involved in stacking interactions. They form homo- and heteroaggregates in solution even at micromolar analytical concentrations (Hamada et al., 1985; Hamada et al., 1991; Mariani et al., 2017; Neumann et al., 2000; Tawarah and Khouri, 1992; Tawarah and Wazwaz, 1993). Aggregation phenomenon can be used in design of silica materials for effective sorptive removal of azo dyes from aqueous solutions. It was expected that introduction of dye-containing functional groups in surface layer of MCM-41 will enhance its sorption affinity to adsorbate due to stacking interactions arising between aromatic rings of dye molecules immobilized on silica surface and supplied from solution. Along with attraction of dye molecules to the chemically immobilized dye-containing sorption centers, the adsorbate-adsorbate interactions, cooperative sorption mechanism can be realized due to the interaction of adsorbate with secondary sorption centers formed on silica surface. In the present work, comparative sorptive removal of acid dye Methyl Red (MR) from individual and binary component solutions with other dyes was carried on mesoporous organosilicas with chemically immobilized 3-aminopropyl and dye-containing surface groups (Scheme 1). We expected that introduction of MR as co-template in sol-gel synthesis of silica material may cause noticeable improvement of structural characteristics of resulting MR_{inc}-NH_2-MCM-41 due to solubilization of azo dye in the micellar aggregates of surfactant (Cho et al., 1981; Gehlen et al., 1995; Hosseinzadeh et al., 2008; Nazar et al., 2010) and have positive influence on sorption of dye molecules in comparison with parent NH_2-MCM-41.

1.   Materials and methods

1.1.   Materials

Tetraethoxysilane ("Merck", ≥ 99%) and (3-aminopropyl)triethoxysilane ("Merck", ≥ 99%) were used

as the silica source in sol-gel and silane synthesis. 1,1′-Carbonyldiimidazole ("Merck", ≥ 98%) was used as coupling agent without preliminary purification. Acid dye Methyl Red ("Reakhim", analytical grade) was dried before coupling procedure in an oven at 373 K for 2 hr. N,N′-dimethylformamide (DMF) ("Reakhim", analytical grade) and ethanol 96% ("Reakhim", chemical grade) were used as solvents. Prior to silane synthesis DMF was dried for 72 hr by use of activated 4 Å molecular sieves, whereas, ethanol 96% was introduced in sol-gel process without additional purification. Hydrochloric acid 37% ("Reakhim", chemical grade) was used along with ethanol 96% for template extraction without preliminary purification. Disubstituted sodium phosphate, monosubstituted potassium phosphate, sodium hydroxide, and phosphoric acid (all from "Reakhim", analytical grade) were used in phosphate buffer preparation as received. Alizarin Yellow (AY) ("Acros", ≥ 96%), Methyl Orange (MO), m-Cresol Purple (MCP), Alizarin Red S (AR), and Eriochrome Black R (ECB) (all from "Reakhim", analytical grade) were dried before sorption studies in an oven at 373 K for 2 hr.

1.2. Experimental methods

Nitrogen low-temperature adsorption-desorption measurements were performed at $T = 77$ K with a Kelvin-1042 Sorptometer. Silica materials were preliminary outgassed under vacuum at 413 K for 20 hr and then analyzed in the region of relative pressures from 0.06 to 0.99 in increment of 0.015. Specific surface area was evaluated by Brunauer-Emmett-Teller (BET) method (Barrett et al., 1951). Pore size distribution was obtained by means of density functional theory (DFT) (Neimark et al., 1998). Pores volume was determined at $p/p_o = 0.99$ (Gregg and Sing, 1967).

X-ray diffraction spectra were collected on a diffractometer DRON-4-02 with monochromatic CuK$_\alpha$ emission ($\lambda = 0.15418$

NH$_2$-MCM-41

MR$_{inc}$-NH$_2$-MCM-41

MR-NH$_2$-MCM-41

Scheme 1 – Surface structure of silica materials prepared by sol-gel synthesis: NH$_2$-MCM-41 — aminopropylsilica; MR$_{inc}$-NH$_2$-MCM-41 — aminopropylsilica synthesized in the presence of MR; MR-NH$_2$-MCM-41 — aminopropylsilica with chemically immobilized MR-containing groups.

nm) and nickel filter. Interplanar distances (d_{100}) were calculated using Bragg diffraction equation (Bragg, 2013). The unit cell parameters (a) were calculated as in paper (Fenelonov et al., 1999).

The transmission electron microscopy (TEM) analysis of mesoporous silicas was performed on a JEM-100CXII electron microscope at 200 kV. Carbon-coated copper grids were used as the silica holders.

FT-IR analysis of synthesized mesoporous silicas was carried out at room temperature using a Thermo Nicollet NEXUS FT-IR spectrophotometer in frequency range from 4,000 to 1,200 cm^{-1} at a spectral resolution of 2 cm^{-1} and 32 scans for each run.

Concentration of amino groups of synthesized silicas was estimated from the results of the potentiometric titration (Belyakova et al., 2006).

UV-Vis absorption spectra of dyes buffer solutions were recorded in 200−800 nm spectral range with a Specord M-40 using quarts cells with 2 or 10 mm path length. An Ionometer I-120.1 calibrated for optimal precision with standard buffer solutions (pH 1.68 and 6.86) was used for pH measuremetns.
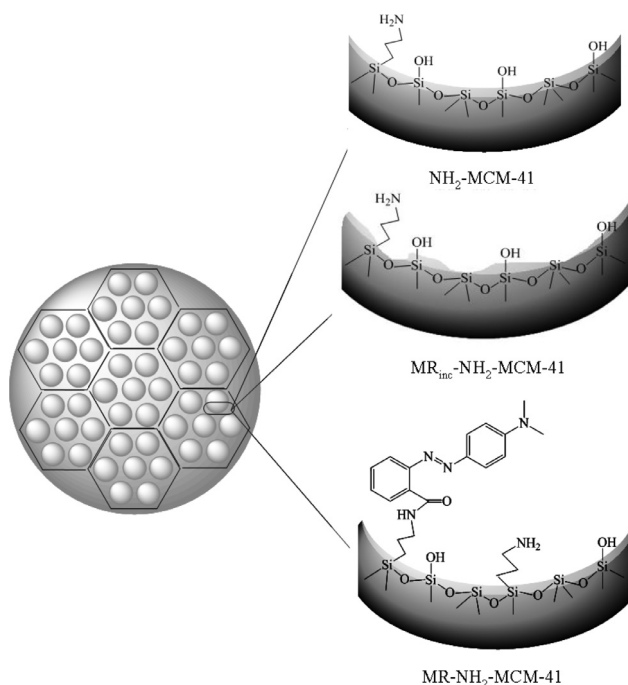
1.3. Adsorbents synthesis

Hexagonally ordered mesoporous silicas NH$_2$-MCM-41 and MR$_{inc}$-NH$_2$-MCM-41 with surface 3-aminopropyl groups were synthesized by base catalyzed sol-gel condensation of structure-forming silanes in the presence of micelles of individual quaternary ammonium salt and its mixture with MR, correspondingly. Briefly, certain amount of CTAB (4.37 g) was placed into a 500 mL conical vessel and dissolved in distilled water (259.2 mL). After that, 25% aqueous ammonium (20.9 mL) or the batch of MR (1.0772 g) dissolved in 25% aqueous ammonium (20.9 mL) was poured into the surfactant solution under vigorous stirring for NH$_2$-MCM-41 and MR$_{inc}$-NH$_2$-MCM-41 synthesis, correspondingly, followed by the addition of silanes mixture (21.5 mL of TEOS and 0.93 mL of APTES). Thereafter, the reaction slurry was stirred at 273 K for 2 hr, transferred into the polypropylene bottle, closed and aged at 373 K without stirring for 24 hr. The precipitated product was washed with deionized water on filter followed by drying in air at 373 K for 2 hr.

At sol-gel synthesis of MR-NH$_2$-MCM-41 silica with surface 3-aminopropyl and MR-containing groups, MR-silane solution in DMF along with TEOS (21.5 mL) was used as silica source. For MR-silane synthesis, the batch of MR (1.0772 g) was dissolved in minimal volume of DMF and treated with solution of CDI (0.6642 g) in DMF. To achieve activation of MR carboxylic group, the reaction mixture was stirred at 293 K for 2 hr. Thereafter, APTES (0.93 mL) was added to the highly reactive imidazolide derivative. After stirring at 293 K for 20 hr the solution was used in sol-gel synthesis of corresponding MR-NH$_2$-MCM-41 silica.

The surfactant as well as molecules of dye physically sorbed in the pore walls of mesoporous silicas was removed by extraction. In general, as-synthesized silica material (1 g) was placed in 250 mL conical vessel, suspended in solution of hydrochloric acid (8 mL) and ethanol (92 mL), and the mixture was stirred at 293 K for 24 hr. Silica particles were separated from solution by filtering and the extraction procedure was repeated two more times. The resulting mesoporous silica was washed thoroughly with deionized water (until the absence of halogen ions and dye in filtrate) and dried in the air at 373 K for 5 hr.

1.4. Sorption studies

In kinetic experiment, series of NH$_2$-MCM-41, MR$_{inc}$-NH$_2$-MCM-41, and MR-NH$_2$-MCM-41 silica batches of 0.01 g were placed in 50 mL glass beakers and 10 mL of 0.06 mmol/L MR solutions in phosphate buffer with pH 4.8 were added. After shaking of prepared suspensions at 293 K for different contact time,

supernatant solutions were separated by filtering through a 0.22 μm PVDF syringe filter and aliquots were taken for UV-Vis spectrophotometric studies. The concentration of dye was determined from optical density of absorption band with maximum at 527 nm. The amount of MR sorbed on silica surface at time t was calculated by formula:

$$A_t = \frac{(C_o - C_t) \cdot V}{m}, \tag{1}$$

where A_t (mmol/g) is the content of MR sorbed on silica surface at time t; C_o (mmol/L) and C_t (mmol/L) are the concentrations of dye at initial moment and at time t, correspondingly; V (L) is the volume of solution; and m (g) is the weight of sorbent used.

Sorption of MR on NH_2-MCM-41, MR_{inc}-NH_2-MCM-41, and MR-NH_2-MCM-41 silicas in dependence of pH was carried out from 0.06 mmol/L phosphate buffer solutions. For this, batches of 0.02 g of silicas and 10 mL of MR phosphate buffer solutions with predetermined pH in the range from 1.0 to 8.0 were placed in 50 mL glass beakers and shaken at 293 K for equilibrium attainment. Then supernatant solutions were separated by filtering through a 0.22 μm PVDF syringe filter and analyzed using UV-Vis spectrophotometer at corresponding wavelengths in the range 530–424 nm. The amount of MR sorbed on silica surface at equilibrium was calculated using calibration curves plotted for each pH value by formula:

$$A = \frac{(C_o - C_{eq}) \cdot V}{m}, \tag{2}$$

where A (mmol/g) is the content of MR sorbed on silica surface at equilibrium; C_o (mmol/L) and C_{eq} (mmol/L) are the concentrations of dye at initial moment and at equilibrium, correspondingly; V (L) is the volume of solution; and m (g) is the weight of sorbent used.

The effect of sorbent dosage on the equilibrium removal of dye was studied in 0.05−0.2 mmol MR solutions in phosphate buffers with pH 4.8. Series of silica sorbents batches of 0.005−0.04 g were placed in 50 mL glass beakers. Then 10 mL of phosphate buffer solution with certain constant concentration of MR and pH were added to each batch and allowed to attain equilibrium at 293 K. The supernatant solutions were collected by filtering through a 0.22 μm PVDF syringe filter and analyzed using UV-Vis spectrophotometer. The concentration of dye was determined from optical density of absorption band with maximum at 527 nm. The amount of MR sorbed on silica surface at equilibrium was calculated as described above.

Sorption of MR on NH_2-MCM-41, MR_{inc}-NH_2-MCM-41, and MR-NH_2-MCM-41 silicas in dependence of equilibrium concentration of dye was carried out from 0.01−0.1 mmol/L MR solutions in phosphate buffers with pH 4.8. For this, batches of 0.01 g of organosilicas and 10 mL of MR phosphate buffer solutions with certain initial concentration were placed in 50 mL glass beakers and shaken at 293 K for equilibrium attainment. Then supernatant solutions were separated by filtering through a 0.22 μm PVDF syringe filter and analyzed using UV-Vis spectrophotometer. The concentration of dye was determined from optical density of absorption band with maximum at 527 nm. The amount of MR sorbed on silica surface at equilibrium was calculated as described above.

Sorptive removal of dyes from individual solutions was performed in phosphate buffer solutions with pH 4.8. For this, batches of 0.01 g of synthesized organosilicas and 10 mL of dyes phosphate buffer solutions with pH 4.8 and initial concentrations of dyes equal to 0.06 and 0.2 mmol/L were placed in 50 mL glass beakers and shaken at 293 K for equilibrium attainment. Then supernatant solutions were separated by filtering through a 0.22 μm PVDF syringe filter and analyzed using UV-Vis spectrophotometer. The amount of dye sorbed on silica surface at equilibrium was calculated from optical density of

absorption band at the wavelength corresponding to the maximum absorbance (527 nm for MR, 375 nm for AY, 468 nm for MO, 438 nm for MCP, 426 nm for AR, 518 nm for ECB) as described above using calibration curves plotted for each individual dye.

The competitive removal of dyes from their binary solutions with 1:1 molar ratio of components by NH_2-MCM-41, MR_{inc}-NH_2-MCM-41, and MR-NH_2-MCM-41 was studied in aqueous and phosphate buffer solutions with pH 4.8. In sorption experiment, batches of 0.01 g of silica materials were placed in 50 mL glass beakers and poured with 10 mL of binary mixtures with initial total concentration of dyes equal to 0.06 mmol/L. The suspensions were shaken at 293 K for equilibrium attainment, whereupon supernatant solutions were separated by filtering through a 0.22 μm PVDF syringe filter and analyzed using UV-Vis spectrophotometer. The equilibrium concentrations of dyes were evaluated using the optical densities at the wavelengths corresponding to the maximum absorbance (527 nm for MR, 375 nm for AY, 468 nm for MO, 438 nm for MCP, 426 nm for AR, 518 nm for ECB):

$$C_1 = \frac{\varepsilon_{2\lambda_1} \cdot A_{\lambda_2} - \varepsilon_{2\lambda_2} \cdot A_{\lambda_1}}{(\varepsilon_{1\lambda_2} \cdot \varepsilon_{2\lambda_1} - \varepsilon_{1\lambda_1} \cdot \varepsilon_{2\lambda_2}) \cdot l}, \tag{3}$$

$$C_2 = \frac{\varepsilon_{1\lambda_1} \cdot A_{\lambda_2} - \varepsilon_{1\lambda_2} \cdot A_{\lambda_1}}{(\varepsilon_{1\lambda_1} \cdot \varepsilon_{2\lambda_2} - \varepsilon_{1\lambda_2} \cdot \varepsilon_{2\lambda_1}) \cdot l}, \tag{4}$$

where C_1 (mmol/L) and C_2 (mmol/L) are the concentrations of dye 1 (AY, MO, MCP, AR, ECB) and dye 2 (MR) at equilibrium, correspondingly; A_{λ_1} and A_{λ_2} are the absorbances of dye 1 and dye 2 at the maximum wavelengths λ_1 and λ_2, correspondingly; $\varepsilon_{1\lambda_1}$ and $\varepsilon_{1\lambda_2}$ are extinction coefficients of dye 1 at the wavelengths λ_1 and λ_2, correspondingly; $\varepsilon_{2\lambda_1}$ and $\varepsilon_{2\lambda_2}$ are extinction coefficients of dye 2 at the wavelengths λ_1 and λ_2, correspondingly; and l (cm) is the length of light path.

The extinction coefficient for each dye at the wavelength of its maximum absorption was calculated from the slope of the linear plot of absorbance against dye concentration. The amounts of dyes sorbed on silica surface at equilibrium were calculated as described above.

To exclude influence of sorption medium and duration of contact on dyes discoloration, blank control experiments were carried out for solutions shaded from exposure to UV radiation by the aluminium foil before sorption studies.

All sorption studies data represent the average values of three runs.

2. Results and discussion

2.1. Characterization of sorbents

The results of low-temperature nitrogen adsorption-desorption experiment used for the characterization of synthesized silica materials are represented in Appendix A Figs. S1, S2. The isotherm of nitrogen adsorption-desorption on NH_2-MCM-41 belongs to the type II with hysteresis loop of the type H3 according to the IUPAC classification (Appendix A Fig. S1). Introduction of MR or MR-silane into the reaction mixture leads to the transformation of isotherm into the type IV with hysteresis loop of the type H3 (Appendix A Fig. S1). A sharp step increase in nitrogen adsorption in a narrow range of relative pressures from 0.25 to 0.35 arising from the capillary condensation in the mesopores is typical for hexagonal mesoporous MCM-41 with uniform pore sizes. The very narrow pore size distributions obtained by means of the DFT method reveal the formation of mesoporous silicas with two most common pore diameters (Appendix A Fig. S2, Table 1). Introduction of MR or MR-silane into the sol-gel synthesis leads to the noticeable changes in mesoporous structure of MR_{inc}-NH_2-MCM-41 and MR-NH_2-MCM-41 silica materials in comparison with NH_2-MCM-41. As can be seen from the

Table 1 – Structural parameters of MCM-41-type silica materials and content of surface 3-aminopropyl groups

Silica	Structural parameters				Content of surface 3-aminopropyl groups		
	S (m²/g)	V (cm³/g)	D (nm)	d_{100}	a	mmol/g	µmol/m²
NH₂-MCM-41	515	0.91	3.93; 5.09	3.93	4.54	0.28	0.54
MR$_{inc}$-NH₂-MCM-41	608	0.80	3.78; 5.09	4.21	4.86	0.29	0.48
MR-NH₂-MCM-41	828	0.72	3.54; 5.29	4.02	4.64	0.18	0.22
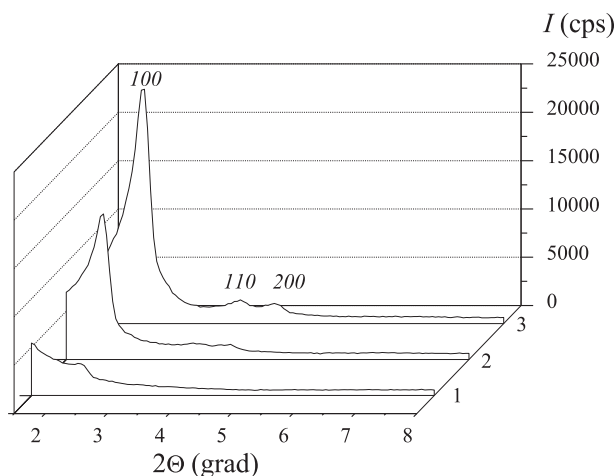
Fig. 1 – X-ray diffractograms of NH₂-MCM-41 (curve 1), MR$_{inc}$-NH₂-MCM-41 (curve 2), and MR-NH₂-MCM-41 (curve 3).

profiles of isotherms, inflection step, corresponding to nitrogen condensation in channels of mesopores, becomes more pronounced (Appendix A Fig. S1). Moreover, decrease of pore diameter and content of larger pores is registered (Appendix A Fig. S2, Table 1). These changes in MR$_{inc}$-NH₂-MCM-41 and MR-NH₂-MCM-41 structure are accompanied with the reducing of hysteresis magnitude (Appendix A Figs. S1, S2, Table 1). Structural parameters of silica sorbents are represented in Table 1. It can be seen that introduction of MR as co-template or MR-silane as structure forming silane in sol-gel synthesis results in noticeable increase of surface area, decrease of total pore volume and narrowing of smaller pore diameters.

The small-angle X-ray diffraction patterns of synthesized organosilica materials are represented in Fig. 1. Only one low intensity reflection from the (100) plane at $2\theta = 2.25$ grad is observed on the diffractogram of NH₂-MCM-41. In contrast, the X-ray diffraction pattern of MR$_{inc}$-NH₂-MCM-41 silica obtained by introduction of MR as co-template in sol-gel synthesis exhibits strong reflection from the (100) plane at $2\theta = 2.1$ grad and two low intensity (110) and (200) peaks at 2θ equal to 3.55, and 4.15 grad, correspondingly, typical of hexagonally arranged pore structure of MCM-41. The X-ray diffraction pattern of MR-NH₂-MCM-41 silica, similarly to the MR$_{inc}$-NH₂-MCM-41 one, shows excellent quality with a strong low-angle peak at 2θ equal to 2.2 grad and two weaker peaks at 2θ equal to 3.75 and 4.3 grad (Fig. 1). However, the intensities of all reflections characteristic for hexagonally arranged mesoporous structure are increased at MR-containing groups introducing into the silica framework. This indicates formation of more uniform hexagonally arranged mesoporous structure in MR-NH₂-MCM-41 compared with NH₂-MCM-41 and MR$_{inc}$-NH₂-MCM-41. For each synthesized silica material, the interplanar distance (d_{100}) corresponding to the (100) plane and unit cell parameters (a) reflecting the spacing between the centers of the adjacent pore

channels (Bragg, 2013; Fenelonov et al., 1999) were calculated (Table 1).

The TEM images of NH₂-MCM-41, MR$_{inc}$-NH₂-MCM-41, and MR-NH₂-MCM-41 silicas are represented in Fig. 2. Visualization of structure proves that synthesized materials possess the highly ordered hexagonal arrays of cylindrical mesopores with uniform size. Obtained results are in a good agreement with the narrow pore size distribution confirmed by low-temperature nitrogen adsorption-desorption data. As can be seen from Fig. 2, entrances to the hexagonally arranged cylindrical mesopores are oriented outside of the silica particles. It is essential for easy accessibility of functional groups located on the internal surface of mesopores for the molecules of adsorbate.

Chemical structure of synthesized mesoporous silicas was confirmed by FT-IR spectroscopy (Fig. 3). As can be seen from the FT-IR spectra of NH₂-MCM-41, MR$_{inc}$-NH₂-MCM-41, and MR-NH₂-MCM-41, the silanol groups involved in adsorption interactions with water molecules produce the broad band around $3,700-3,000$ cm⁻¹ attributed to the valence vibrations of the O–H bonds (Fig. 3). It overlaps the absorption peak related to the N–H stretching vibrations in 3-aminopropyl group which are expected in the region $3,300-3,000$ cm⁻¹. The absorption bands corresponding to the C–H stretching vibrations in the CH₂ and CH₃ groups of surface 3-aminopropyl groups are registered at $3,000-2,500$ cm⁻¹ (Fig. 3). Noticeable contribution in their intensity in the FT-IR spectrum of MR-NH₂-MCM-41 belongs to the stretching vibrations of the C–H bonds in the CH₃ groups of chemically immobilized MR-containing groups (Fig. 3, curve 3). Comparative analysis of position of absorption bands located in low-frequency region of FT-IR spectra proves that NH₂-MCM-41 and MR$_{inc}$-NH₂-MCM-41 have similar chemical structure of surface layer. The characteristic absorption band at 1,570 cm⁻¹ is indicative of the N–H bending modes of the primary amino groups, which are present in both synthesized mesoporous silicas. The absorption bands corresponding to the deformation vibrations of the C–H bonds in the CH₂ and CH₃ groups of 3-aminopropyl groups are registered at 1,472, 1,448, 1,390 cm⁻¹. Chemical immobilization of MR-containing functional groups on silica surface causes noticeable changes in the FT-IR spectrum of MR-NH₂-MCM-41 compared with NH₂-MCM-41 and MR$_{inc}$-NH₂-MCM-41. The substantial enhancement of intensity of the absorption band at $1,800-1,580$ cm⁻¹ is mainly associated with the contribution of the C=O stretching vibrations of amide bond. At the same time, distinct peak with maximum at 1,604 cm⁻¹ is appeared in the FT-IR spectrum of MR-NH₂-MCM-41. It can be assigned to the valence vibrations of the C=C bonds in the benzene rings. The absorption band at 1,560 cm⁻¹ is indicative of the N–H bending modes of formed amide bond. Whereas, the band with maximum at 1,527 cm⁻¹ appears due to the C–N stretching vibrations in the chemically immobilized MR-containing groups. The absorption bands with maxima at 1,448, 1,400, and 1,370 cm⁻¹ belong to the deformation vibrations of the C–H bonds in the CH₂ and CH₃ groups as well as the valence vibrations of the C=C bonds in the benzene rings (Fig. 3, curve 3). Observed changes in the FT-IR spectrum of MR-NH₂-MCM-41 compared with NH₂-MCM-41 and MR$_{inc}$-NH₂-MCM-41
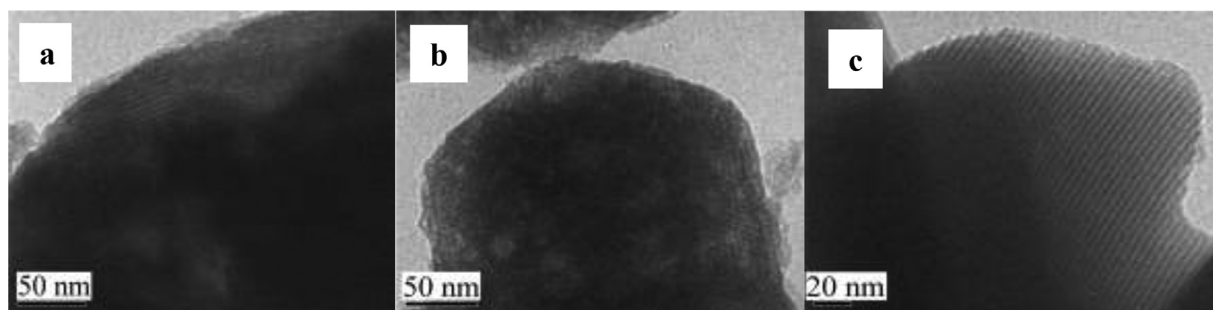
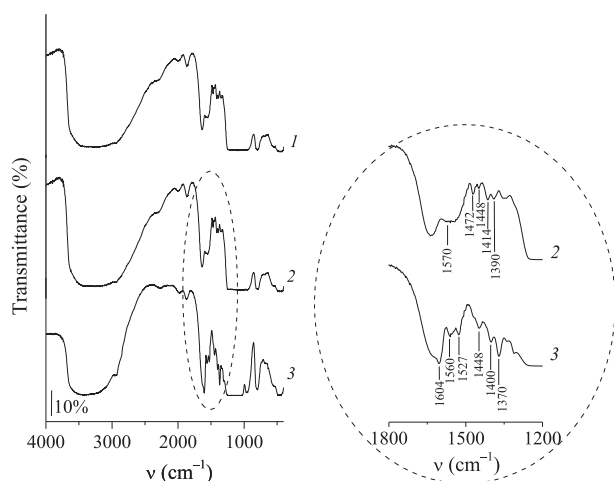**Fig. 2 – TEM images of NH$_2$-MCM-41 (a), MR$_{inc}$-NH$_2$-MCM-41 (b), and MR-NH$_2$-MCM-41 (c).**

Fig. 3 – Transmittance FT-IR spectra of NH$_2$-MCM-41 (curve 1), MR$_{inc}$-NH$_2$-MCM-41 (curve 2), and MR-NH$_2$-MCM-41 (curve 3).

give proofs of dye moieties presence in synthesized organosilica.

Content of 3-aminopropyl groups in surface layer of synthesized organosilicas was determined from the results of the potentiometric titration (Belyakova et al., 2006) and represented in Table 1.

As it was proved by low-temperature nitrogen adsorption-desorption, x-ray diffraction, and TEM studies, all synthesized silica materials possess hexagonally arranged mesoporous structure accessible to the adsorbate molecules. However, different structural parameters and chemical composition of surface layer, which were attained by addition of MR as co-template or MR-silane as structure forming silane in sol-gel synthesis of MR$_{inc}$-NH$_2$-MCM-41 and MR-NH$_2$-MCM-41, may influence sorption ability of these materials towards MR and other dyes noticeably in comparison with NH$_2$-MCM-41 as reference material.

2.2. Sorptive removal of dyes from single and binary solutions by organosilicas

Understanding the solubility limits of MR is required for sorption studies. As shown by preliminary experiments, MR solutions transparent in all range of pH values can be prepared in ethanol. But, sorptive removal of dye from alcohol medium is extremely low and cannot be used for assessment of organosilica sorbents effectiveness. Addition of water or phosphate buffer in ethanol solutions enhances the flocculation process substantially. The most pronounced self-aggregation of MR

is observed in aqueous environment, turbidity of 0.5 mmol/L MR solutions in water or phosphate buffer increases considerably in comparison with alcohol medium. It should be mentioned that decrease of pH from 4.8 to 4.2 promotes the self-aggregation process. Taking into account tendency of MR to flocculate, especially in weakly acidic environment, all sorption studies were carried out using dye solutions with concentrations less than or equal to 0.2 mmol/L, which do not contain aggregates able to influence the accuracy of UV-Vis spectrophotometric assessment of sorption process.

Variation of solution pH value causes changes in degree of dissociation of adsorbate molecules as well as surface functional groups of silica sorbents (Appendix A Fig. S3, Fig. 4). Therefore, removal of dye molecules from aqueous solutions can be successfully controlled by carrying out sorption process at a suitable acidity of the medium. Sorptive removal of MR by synthesized silica materials was studied from diluted solutions in phosphate buffer with pH from 1 to 8 (Fig. 5). It can be seen that sorption of MR on NH$_2$-MCM-41 and MR$_{inc}$-NH$_2$-MCM-41 silicas is highly pH-dependent. Increase of solution pH from 1 to 2.5 leads to the sharp rise of MR removal. The maximal values of MR uptake are attained in the pH range from 2.5 to 5. Such character of MR sorption can be explained by hydrogen bonding with participation of silanol groups and increasing amounts of nonprotonated 3-aminopropyl groups of NH$_2$-MCM-41 and MR$_{inc}$-NH$_2$-MCM-41 with basic centers (dimethylamino group and nitrogen of azo linkage) and carboxylic group of MR, correspondingly (Appendix A Fig. S3, Fig. 4). Accumulation of negative charge on NH$_2$-MCM-41 and MR$_{inc}$-NH$_2$-MCM-41 surfaces, which takes place at higher pH values due to the ionization of silanol groups, does not favor sorption of MR anions and is accompanied with drastic decrease of MR removal efficiency from phosphate buffer solutions (Fig. 5). The profile of the pH dependence of MR sorption by silica with chemically immobilized dye moieties differs noticeably from that ones obtained for NH$_2$-MCM-41 and MR$_{inc}$-NH$_2$-MCM-41. As can be seen from Fig. 5, substantial increase of MR uptake by MR-NH$_2$-MCM-41 is observed over a wide range of pH values. Obviously, in addition to the hydrogen bonding, cooperative interactions of adsorbate with MR-NH$_2$-MCM-41 surface have an impact on sorption process. Likewise sorption of MR on NH$_2$-MCM-41 and MR$_{inc}$-NH$_2$-MCM-41 silicas, substantial decrease of dye removal by MR-NH$_2$-MCM-41 is observed at pH values higher than 6.5 due to electrostatic repulsion between ionized surface silanol groups and negatively charged anions of MR (Fig. 5).

In accordance with the obtained results, effective removal of MR from phosphate buffer solutions takes place at pH values within a range of 2.5–5. Therefore, all further studies of influence of sorbent dosage, duration of contact, and equilibrium concentration of dye on sorption efficiency of synthesized silica materials were carried out in weakly acidic medium.

As synthesized silica materials have commensurable structural parameters and similar surface functional groups (silanol and 3-aminopropyl), the effect of sorbent dosage on the ex-
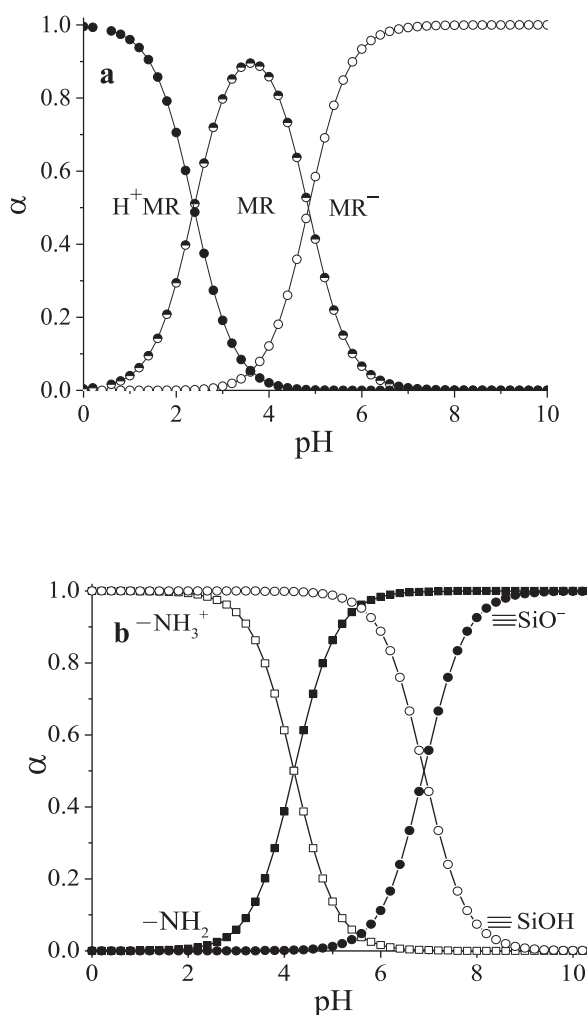
Fig. 5 – Effect of pH on MR removal by NH_2-MCM-41 (curve 1), MR_{inc}-NH_2-MCM-41 (curve 2), and MR-NH_2-MCM-41 (curve 3) from phosphate buffer solutions (batch of sorbent − 0.02 g, initial concentration of dye − 0.06 mmol/L).

Fig. 4 – Distribution of protolytic forms of MR (a) as well as surface silanol and 3-aminopropyl groups of silica materials (b) as a function of pH.

Fig. 6 – Effect of NH_2-MCM-41 dosage on MR removal from phosphate buffer solution with initial concentration of dye equal to 0.06 mmol/L at pH 4.8.

tent of MR removal from its phosphate buffer solution with pH 4.8 was studied using NH_2-MCM-41 as reference material. In weakly acidic solutions silanol as well as 3-aminopropyl groups participate in sorption of MR (Appendix A Fig. S3, Fig. 4). Removal of dye from phosphate buffer solution with pH 4.8 reaches 59% at adsorbent dosage equal to 0.5 g/L (Fig. 6). Subsequent rise of NH_2-MCM-41 content leads to the negligible increase of MR sorption.

The kinetic studies were carried out to estimate the contact time required for the attainment of sorption equilibrium as well as reveal the mechanism of interactions between the sorbents and adsorbate. The effect of contact time on the removal of MR by synthesized organosilica sorbents from phosphate buffer solutions with pH 4.8 in static and dynamic conditions is represented in Fig. 7. It can be seen that the sorption rate is increased rapidly at the beginning of the process and becomes slower at reaching near the equilibrium conditions. At the initial contact time large dye concentration gradient induces the interaction of MR with accessible higher-energy sorption sites. But, sorption rate drops significantly with the time due to decrease of dye concentration in solution, diffusion of MR molecules deeper into the pore volume of sorbent, and occupation of lower-energy sites.

Comparison of kinetic curves demonstrates that the efficiency of MR removal by NH_2-MCM-41, MR_{inc}-NH_2-MCM-41,
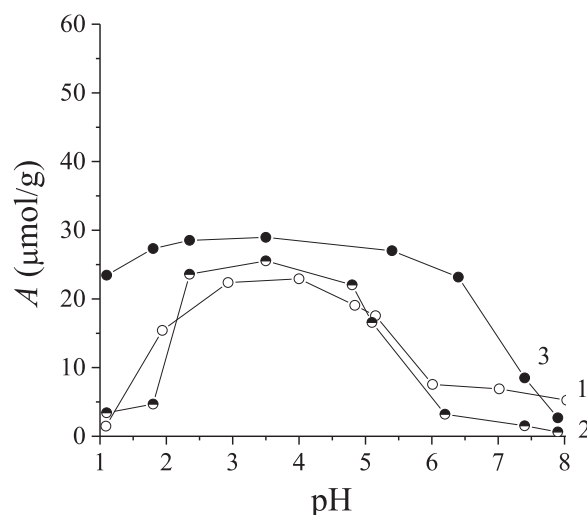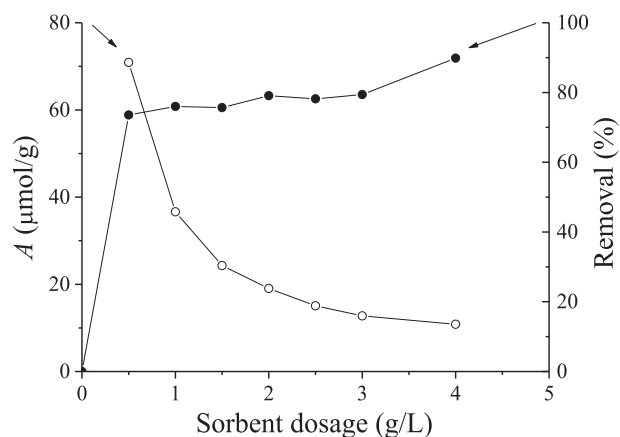
and MR-NH_2-MCM-41 silicas from phosphate buffer solutions with pH 4.8 is somewhat lower in static conditions than in dynamic ones throughout the duration of kinetic experiment (Fig. 7). Despite of the existence of plateau regions on all kinetic curves, the equilibrium sorption capacities of organosilica materials, which are attained for dye sorption in dynamic conditions, are not reached in static ones (Fig. 7). Taking into account tendency of MR for self-aggregation in weakly acidic solutions, it can be supposed that the lower values of MR sorption in static conditions may be caused by preferential sorption of dye molecules on the external surface of sorbents accompanied with agglomeration of MR molecules and partial blocking of pore entrances. Agitation of suspensions provides more uniform distribution of sorbed MR molecules on the surface of silica materials and results in higher removal efficiency.

Several kinetic models such as pseudo-first order Lagergren, pseudo-second order Ho-McKay, and intraparticle diffusion Weber-Morris were used to analyze sorption kinetic behavior of MR on silica materials and clarify the mechanism of sorption
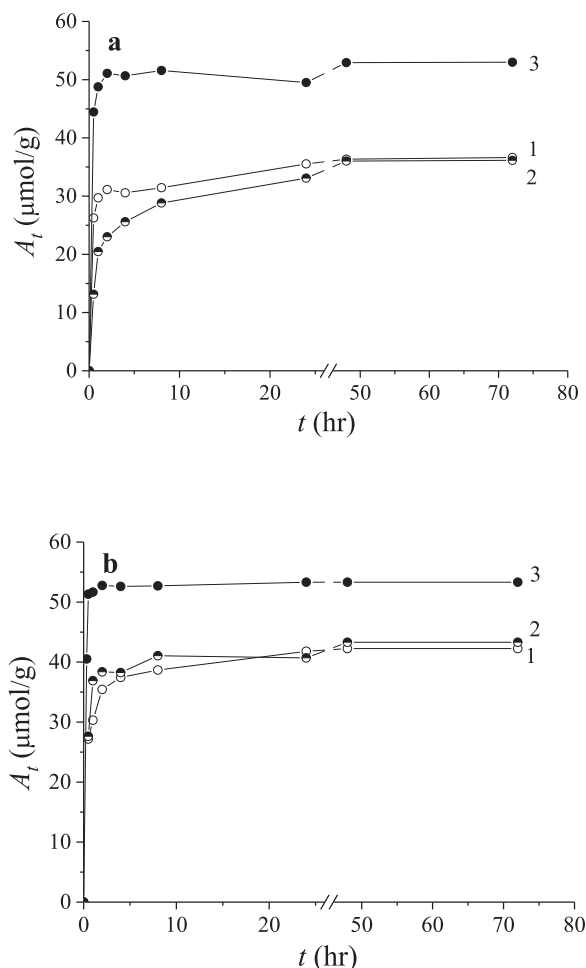
Fig. 7 – Effect of contact time on MR removal by NH$_2$-MCM-41 (curve 1), MR$_{inc}$-NH$_2$-MCM-41 (curve 2), and MR-NH$_2$-MCM-41 (curve 3) from phosphate buffer solutions with initial concentration of dye equal to 0.06 mmol/L in static (a) and dynamic (b) conditions at pH 4.8.

process. The values of rate constants and equilibrium sorption of MR from phosphate buffer solutions with pH 4.8 were determined using the linear expressions of pseudo-first and pseudo-second order kinetic equations (Table 2). The best agreement of experimental results and the model predicted values was selected based on the comparison of linear regression correlation coefficients (R^2). As can be seen from Table 2, correlation coefficients calculated for the linear plots using pseudo-second order kinetic model have higher values than that obtained using pseudo-first one. In addition, theoretical values of A_{eq} estimated by Lagergren equation differ significantly from the experimental ones (Table 2). Obviously, the pseudo-first order model is not suitable to describe the experimental kinetic profiles. Hence, sorption process of MR on synthesized materials follows the pseudo-second order kinetic model (Appendix A Fig. S4).

Diffusion of dye molecules into the pore volume of silica material is often the rate-limiting step of sorption process. Therefore, the contribution of intraparticle diffusion was assessed using the Weber-Morris equation (Weber and Morris, 1963) (Table 2). The plot of A_t versus $t^{1/2}$ should be a straight line with slope and intercept equal to k_t and C, correspondingly. According to the applied model, intraparticle diffusion is the rate-controlling step of sorption if the line plotted in the

coordinates of the Weber-Morris equation passes through the origin. However, as can be seen from Appendix A Fig. S5, the kinetic data plotted in coordinates of Weber-Morris equation are not linear over the whole time range. The multi-linear character of the Weber-Morris plots proves that the MR sorption on MCM-41-type silicas has complex nature. The first segment is attributed to the rapid outer diffusion of dye molecules from solution to the external surface of the sorbent. The second one describes the intra-particle diffusion, which takes place at moving of MR molecules from external surface of silica sorbent to the internal pore surface. The last segment is assigned to the equilibrium stage of sorption, for which deceleration of intra-particle diffusion is registered due to the filling of surface sorption centers and decrease of dye concentration in solution. The effect of boundary layer on MR sorption by MCM-41-type silicas is increased noticeably when static conditions are changed by dynamic ones at pH 4.8 (Table 2). Obviously, contribution of surface sorption into the rate-limiting step increases at agitating of suspensions (Table 2). Dynamic conditions promote the outer diffusion as well as diffusion of dye molecules in pore volume of sorbents particles. The rate of outer diffusion in dynamic conditions increases in the range NH$_2$-MCM-41 < MR$_{inc}$-NH$_2$-MCM-41 < MR-NH$_2$-MCM-41. Whereas, the intraparticle diffusion rate for MR$_{inc}$-NH$_2$-MCM-41 is higher than for MR-NH$_2$-MCM-41 (Table 2). This effect can be related with more arranged mesoporous structure of MR$_{inc}$-NH$_2$-MCM-41 synthesized in the presence of MR as co-template as well as with partial blocking of pore entrances in MR$_{inc}$-NH$_2$-MCM-41 and MR-NH$_2$-MCM-4 nanoparticles that takes place at sorption of dye on the external surface of organosilica. Analysis of Weber-Morris plots indicates that the rates of mass transfer in the initial and final steps of MR sorption differ substantially, and the intraparticle diffusion is not the only one mechanism controlling the rate of MR sorptive removal by synthesized silica materials in weakly acidic solutions.

The relationship between the equilibrium concentrations of adsorbate in solution and on the surface of sorbent at constant temperature has fundamental importance in description of sorption process. Isotherms were obtained at pH 4.8 where sorption efficiency of synthesized materials is highest due to the large number of interactions between dye and surface sites of silicas. At studied pH value silanol groups of sorbents are nonionized (Fig. 4) and can participate in hydrogen bonding with basic centers as well as with any protolytic form of carboxylic group of MR. Surface 3-aminopropyl groups are partially protonated (Fig. 4). Near by 20% of them bare positive charge at pH 4.8 and are able to form hydrogen bonds with dissociated carboxylic groups of MR. Whereas, the rest of 3-aminopropyl groups are nonprotonated and have high electron density on nitrogen atom. So, they can interact only with nondissociated carboxylic groups of MR, which content is equal to 47% at pH 4.8 (Fig. 4).

As can be seen from Fig. 8, silica materials have different sorption efficiency at low MR equilibrium concentrations. It results from the different affinity between sorbents and dye molecules. The surface of NH$_2$-MCM-41 and MR$_{inc}$-NH$_2$-MCM-41 contains two types of functional groups (silanol and 3-aminopropyl), which are able to interact with MR through hydrogen bonds formation. Their contribution to the sorption process is relatively small. Therefore, the quantity of sorbed dye rises slowly until the attainment of dye equilibrium concentration equal to 0.012 mmol/L, whereupon sorption efficiency of NH$_2$-MCM-41 and MR$_{inc}$-NH$_2$-MCM-41 increases drastically. Contrary situation is observed for silica with chemically immobilized MR-containing moieties (Fig. 8). Efficient removal of dye by MR-NH$_2$-MCM-41 is already occurred in the low equilibrium concentrations region. In both cases sharp rise of MR sorption isotherms can be explained by π–π stacking interactions arising between aromatic systems of adsorbed or chem-

Table 2 – Kinetic parameters for MR sorption on MCM-41-type silicas in static and dynamic (bold) conditions at pH 4.8 calculated using pseudo-first and pseudo-second order kinetic models as well as the intraparticle diffusion model

Kinetic model	Lagergren			Ho-McKay			Weber-Morris		
Linear form of equation	$lg(A_{eq} - A_t) = lgA_{eq} - \frac{k_1}{2.303}t$			$\frac{t}{A_t} = \frac{1}{k_2 A_{eq}^2} + \frac{1}{A_{eq}}t$			$A_t = k_t \cdot t^{1/2} + C$		
Kinetic parameters	k_1	A_{eq}	R^2	k_2	A_{eq}	R^2	k_t	C	R^2
NH$_2$-MCM-41	0.079	10.55	0.923	0.044	36.48	0.999	22.87	3.93	0.929
							1.39	28.26	0.939
							0.32	34.03	0.984
	0.201	**18.37**	**0.982**	**0.050**	**42.57**	**0.999**	**25.50**	**3.34**	**0.958**
							1.50	**34.44**	**1.000**
							0.13	**41.20**	**0.900**
MR$_{inc}$-NH$_2$-MCM-41	0.103	21.24	0.980	0.018	36.81	0.999	17.02	0.87	0.982
							2.49	21.09	0.987
							0.08	35.46	1.000
	0.137	**13.34**	**0.927**	**0.047**	**43.49**	**0.999**	**28.57**	**3.43**	**0.956**
							14.42	**19.30**	**0.879**
							0.73	**37.61**	**0.926**
MR-NH$_2$-MCM-41	0.086	7.04	0.790	0.061	53.02	0.999	37.42	6.87	0.921
							0.36	49.74	0.646
	0.144	**2.30**	**0.834**	**0.451**	**53.36**	**1.000**	**71.84**	**0.03**	**0.999**
							2.11	**49.72**	**0.981**
							0.11	**52.53**	**0.887**

A_{eq} (μmol/g) and A_t (μmol/g) are sorption capacities at equilibrium and at time t; k_1 (1/hr) and k_2 (g/μmol·hr) are rate constants of pseudo-first and pseudo-second order sorption processes; k_t (μmol/g·hr$^{1/2}$) is intraparticle diffusion rate constant; C is constant providing information about the thickness of the boundary layer.
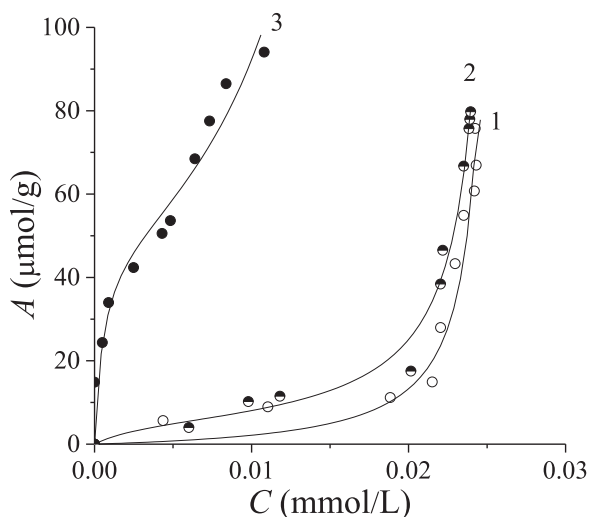

Fig. 8 – Isotherms of MR sorption by NH$_2$-MCM-41 (curve 1), MR$_{inc}$-NH$_2$-MCM-41 (curve 2), and MR-NH$_2$-MCM-41 (curve 3) from phosphate buffer solutions with pH 4.8 (batch of sorbent — 0.01 g, initial concentration of dye — 0.01–0.1 mmol/L): points represent the experimental results, whereas lines are calculated by nonlinear regression analysis of BET equation.

ically immobilized moieties of dye and supplied from solution ones (Scheme 2). Obtained results demonstrate the key role of cooperative interactions in sorptive removal of MR from diluted aqueous solutions. MR-NH$_2$-MCM-41 silica was regenerated by sequential washing with ethanol solution acidified by hydrochloric acid and water. Equilibrium adsorption experi-

ment was repeated two more times and proved that studied organosilica retains nearby 87% of adsorption capacity.

In this study, the detailed analysis of equilibrium sorption data was carried out using four widely applied isotherm models: Langmuir, Freundlich, Redlich-Peterson, and Brunauer-Emmett-Teller (BET).

The Langmuir isotherm model assumes MR sorption on energetically equivalent sorption sites of silica materials. According to the Langmuir isotherm model, saturation point is attained at monolayer formation and no further sorption can be realized as all sites are occupied by dye molecules. The Freundlich isotherm theory can be applied to the heterogeneous surface with non-equivalent sorption sites. The Freundlich isotherm is valid over a certain range of equilibrium concentrations only. It cannot be used for a straight linear part of isotherm occurring either at low (the value of n should be assumed equal to 1) or at high concentrations of adsorbate (the isotherm increases unreservedly, but the surface has a limited value and it must be in the condition of saturation). To estimate sorption parameters, the linear forms of Langmuir and Freundlich equations were used (Table 3). The sorption mechanism of Redlich-Peterson model follows a non ideal monolayer sorption and combines features of both the Langmuir and Freundlich equations. The Redlich-Peterson model can predict sorption either on heterogeneous or homogenous sites of silica surface for which the mechanism of sorption has hybrid character. The classical BET isotherm model describes multilayer sorption from the gas phase. Therefore, its direct application for liquid-solid phase process leads to erroneous results. In the present paper, corrected form of the BET equation proposed by authors (Ebadi et al., 2009; Gritti and Guiochon, 2003) was used for modelling sorption of MR on silica surface from phosphate buffer solutions. At consideration of liquid–solid sorption of dye from the point of view of BET model, it is assumed that the solvent is weakly sorbed on silica surface, whereas solute is strongly sorbed. Molecules of dye adsorbate in the first layer serve as sorption sites for the second layer, and so on. Sorption
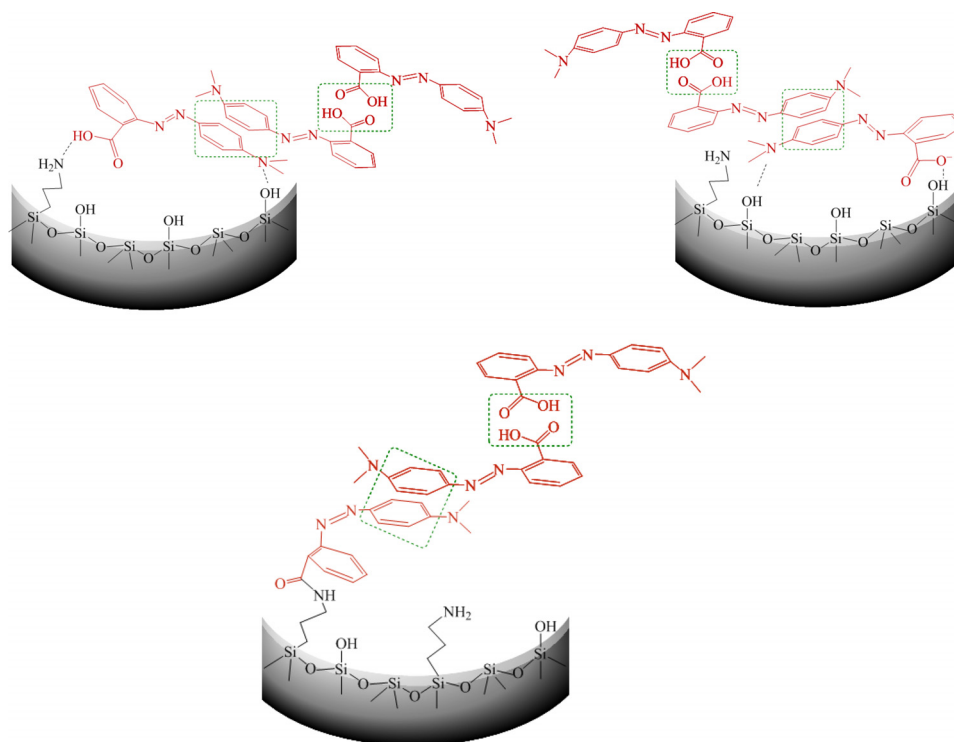
Scheme 2 – Cooperative interactions of MR supplied from solution with adsorbed or chemically immobilized on silica surface moieties of dye.

Table 3 – Parameters of MR equilibrium sorption on MCM-41-type silicas at pH 4.8 calculated using the Langmuir and Freundlich models

Equilibrium sorption model	Langmuir			Freundlich		
Linear form of equation	$\frac{C_{eq}}{A_{eq}} = \frac{1}{K_L A_m} + \frac{C_{eq}}{A_m}$			$lgA_{eq} = lgK_F + \frac{1}{n}lgC_{eq}$		
Sorption parameters	K_L	A_m	R^2	K_F	n	R^2
NH_2-MCM-41	6.05	253.16	0.066	6746.52	0.73	0.799
MR_{inc}-NH_2-MCM-41	480.62	0.07	0.884	$2.46 \cdot 10^5$	0.45	0.918
MR-NH_2-MCM-41	618.83	93.63	0.094	567.47	2.39	0.973

A_{eq} (μmol/g) is the amount of dye sorbed on silica surface; C_{eq} (mmol/L) is the concentration of dye remaining in the solution after equilibrium attainment; A_m (μmol/g) is the amount of dye required to form monolayer on the sorbent surface; K_L (L/μmol) is the constant related to the affinity of the binding sites; K_F and n (1/g) are the Freundlich constants; $1/n$ is the measure of sorption intensity, which can be between 0 and 1.

parameters of Redlich-Peterson and BET equations obtained from nonlinear regression analysis are represented in Table 4.

The results obtained from the analysis of experimental isotherms using equilibrium sorption models prove that the values of correlation coefficients (R^2) increase at transition from Langmuir model to the Freundlich, Redlich-Peterson and BET ones (Tables 3, 4). Noticeable difference between R^2 values calculated by Langmuir and Freundlich models indicates a pronounced heterogeneous nature of MR sorption on NH_2-MCM-41, MR_{inc}-NH_2-MCM-41, and MR-NH_2-MCM-41. It should be noted that the correlation coefficients estimated by Redlich-Peterson and BET models have close values in some cases. This fact proves ambiguous nature of MR sorption on organosilicas due to the formation of hydrogen bonds between different protolytic forms of surface functional groups of silica sorbents and MR as well as $\pi - \pi$ stacking interactions arising between aromatic systems of sorbed or chemically immobilized moieties of dye and supplied from solution ones. The highest values of correlation coefficients were obtained at applying of BET model

to the description of MR sorption on synthesized organosilica materials (Fig. 8, Tables 3, 4). According to the BET model, molecules in the second and subsequent layers are behaved essentially as those in the bulk liquid. Therefore, it can be presumed that cooperative interactions play crucial role in sorptive removal of MR from phosphate buffer solutions by NH_2-MCM-41, MR_{inc}-NH_2-MCM-41, and MR-NH_2-MCM-41.

In accordance with the BET model, adsorption capacity of MR-NH_2-MCM-41 achieved at contact with phosphate buffer solution of MR (pH 4.8, concentration of dye up to 0.1 mmol/L) is equal to 47.89 mg/g. This value is higher or commensurable with the adsorption capacities of other widely used sorbents used for sorption removal of MR. In particular, adsorption capacity of activated carbon in relation to MR varies from 31.65 mg/g (Santhi et al., 2009) to 46.29 mg/g (Ghaedi et al., 20110), whereas in the case of SiO_2-coated Fe_3O_4 magnetic nanoparticles it reaches 49.50 mg/g (Shariati-Rad et al., 2014). Equilibrium sorption studies realized in this work were limited by range of concentrations in which MR does not form aggregates

Table 4 – Parameters of MR equilibrium sorption on MCM-41-type silicas at pH 4.8 calculated using the Redlich-Peterson and BET models

Equilibrium sorption model	Redlich-Peterson				Brunauer-Emmett-Teller			
Equation	$A_{eq} = \dfrac{K_R C_{eq}}{1 + a_R C_{eq}^B}$				$A_{eq} = \dfrac{A_m K_S C_{eq}}{(1 - K_L C_{eq})(1 - K_L C_{eq} + K_S C_{eq})}$			
Sorption parameters	K_R	a_R	B	R^2	K_S	K_L	A_m	R^2
NH$_2$-MCM-41	150	−39.15	1	0.983	30.40	39.14	3.91	0.982
MR$_{inc}$-NH$_2$-MCM-41	225	−15.36	0.75	0.985	38.74	331.69	5.84	0.988
MR-NH$_2$-MCM-41	9856	−9.59	1	0.909	1839	49.44	47.89	0.984

K_R (L/g) and a_R (L/mmol) are the Redlich-Peterson isotherm constants; β is exponent that lies between 0 and 1 (sorption model follows the Langmuir model when β value is 1, while when β value is 0, the sorption model follows the Henry's law); K_S (L/mmol) is term for the energy of interaction with the surface; K_L (L/mmol) is the equilibrium constant for surface sorption-desorption.

able to influence the accuracy of UV-Vis spectrophotometric measurements. Taking into account form of isotherm (Fig. 8), it can be supposed that MR-NH$_2$-MCM-41 silica may demonstrate higher sorption ability at application in more concentrated solutions.

To estimate effectiveness of synthesized silica materials, sorption of different dyes was studied from their single and binary component systems with MR at given initial concentration of dyes in phosphate buffer solutions with pH 4.8 (Appendix A Fig. S6, Table S1). The substances chosen for sorption studies belong to the acidic dyes, whose −COOH (AY) or -SO$_3$H (MO, ECB, MCP, AR) groups are fully dissociated at pH 4.8, whereas carboxylic groups of MR have relatively high value of pK_a and exist in partially dissociated state. Comparative analysis of dyes sorptive removal by organosilica materials was carried out taking into account the pK_a values of other functional groups (-N=N-, -OH), which can undergo acid-base dissociation at the conditions of experiment (Appendix A Table S1).

The amounts of dyes sorbed by organosilica materials were calculated from optical densities of absorption bands at the wavelengthes corresponding to the maximum absorbances using calibration curves plotted for each individual dye (Appendix A Fig. S6, Table S1). The sorption capacities attained at equilibrium were considered as crucial parameters for estimation of sorbents selectivity effectiveness. Sorption measurements carried out in single component systems clearly reveal that NH$_2$-MCM-41 and MR$_{inc}$-NH$_2$-MCM-41 silicas have equivalent equilibrium sorption ability in relation to MR in diluted solutions (Fig. 9). Taking into account protolytic properties of this dye, it can be seen that MR is in partially dissociated form at pH 4.8 (Fig. 4, Appendix A Table S1). So, the main contribution in sorption belongs to the numerous hydrogen bonds arising between functional groups of MR and surface 3-aminopropyl or silanol groups of NH$_2$-MCM-41 and MR$_{inc}$-NH$_2$-MCM-41 as well as cooperative interactions of MR supplied from solution with sorbed on silica surface moieties of dye (Scheme 2). Contrary effect is observed for the rest of dyes, whose sorptive removal by MR$_{inc}$-NH$_2$-MCM-41 is noticeably lower than by NH$_2$-MCM-41. It can be explained by the influence of MR, which was used as co-template in sol-gel synthesis of MR$_{inc}$-NH$_2$-MCM-41, on mesoporous structure formation.

As can be seen from Fig. 9, different nature of interactions of functional groups lining surface of organosilica materials with adsorbate leads to the increase of sorption values of preferential majority of acid dyes on MR-NH$_2$-MCM-41 surface in comparison with NH$_2$-MCM-41 and MR$_{inc}$-NH$_2$-MCM-41 from single component solutions in phosphate buffer with pH 4.8. The efficiency of some dyes sorptive removal is increased in several times at rise of MR initial concentration from 0.06 to 0.2 mmol/L (Fig. 9). It can be supposed that along with hydrogen bonding arising between functional groups of dyes and sur-
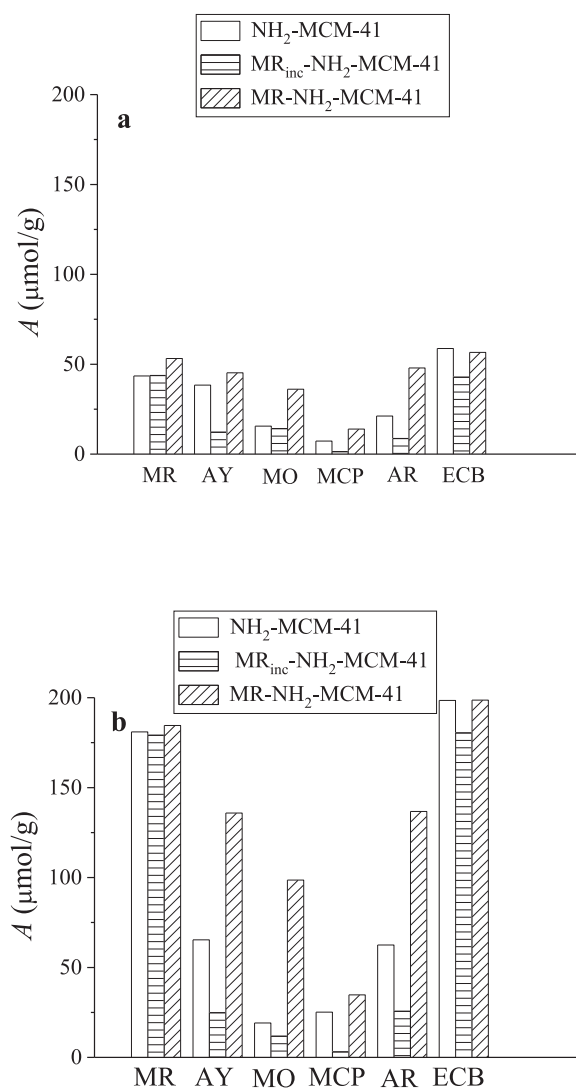

Fig. 9 – Removal of dyes by NH$_2$-MCM-41 (open bars), MR$_{inc}$-NH$_2$-MCM-41 (horizontal stripes), and MR-NH$_2$-MCM-41 (diagonal stripes) from their single component systems in phosphate buffer solutions with initial concentrations of dyes equal to 0.06 mmol/L (a) and 0.2 mmol/L (b) at pH 4.8.
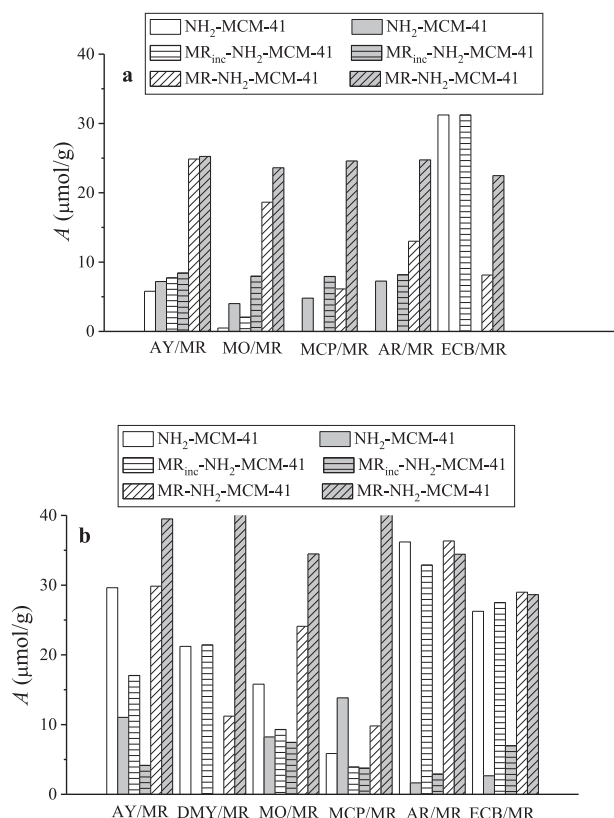
Fig. 10 – Removal of dyes (white) and MR (grey) by NH$_2$-MCM-41 (open bars), MR$_{inc}$-NH$_2$-MCM-41 (horizontal stripes), and MR-NH$_2$-MCM-41 (diagonal stripes) from their binary mixtures (1:1 molar ratio) in phosphate buffer solutions with initial total concentrations of dyes equal to 0.06 mmol/L at pH 4.8 (a) and in aqueous solutions with initial total concentrations of dyes equal to 0.06 mmol/L at pH 5.5 (b).

face silanol or 3-aminopropyl groups of MR-NH$_2$-MCM-41, $\pi-\pi$ stacking interactions between aromatic systems of chemically immobilized MR-containing groups or adsorbed dye molecules and supplied from solution ones take place.

In order to explore the selective sorption of dyes by synthesized silica materials, binary component solutions with initial total concentration of dyes equal to 0.06 mmol/L were prepared in phosphate buffer with pH 4.8 and used in sorption studies. Comparison of the obtained results proves that sorptive removal of all dyes is reduced in binary mixtures: total sorption for each studied binary system is lower than sum of dyes sorption values attained in single component solutions (Figs. 9 and 10a). Obviously, components of binary mixtures are involved in competitive binding with available surface sites of silica materials. It should be noted that removal of MR from all studied mixtures except for ECB-containing one is prevailing. In the case of MCP/MR and AR/MR systems presence of MR completely suppresses sorption of another component of the mixture (Fig. 10a). As it was mentioned above, the key role in removal of MR by NH$_2$-MCM-41 and MR$_{inc}$-NH$_2$-MCM-41 from solutions in phosphate buffer with pH 4.8 belongs to the numerous hydrogen bonds and $\pi-\pi$ stacking interactions. Taking into account somewhat higher sorption of MR on MR$_{inc}$-NH$_2$-MCM-41 in comparison with NH$_2$-MCM-41, it can be supposed that geometry of adsorbate molecules as well as peculiarities of mesoporous structure caused by introduction of MR as co-template in sol-gel synthesis of MR$_{inc}$-NH$_2$-MCM-41 has

noticeable influence on sorption selectivity. Grafting of MR-containing groups on silica surface facilitates sorptive removal of dyes due to $\pi-\pi$ stacking interactions arising between aromatic systems of chemically immobilized dye moieties and supplied from solution ones.

Drastic changes in sorption selectivity of synthesized organosilica materials may be achieved by variation of solution acidity. It was supposed that at pH values higher than the pK_a of MR, sorption of MR may be less favorable as compared to the anions of other dyes. In addition, sorption process may be influenced by phosphate buffer medium. To elucidate the affect of MR protolytic state on its selective removal by organosilica materials, sorption of MR was carried out from binary component water solutions at pH 5.5 (Appendix A Fig. S6). It was found that sorptive removal of MR by NH$_2$-MCM-41 and MR$_{inc}$-NH$_2$-MCM-41 from water solutions with pH 5.5 proceeds less effectively mainly due to the weak hydrogen bonding of increasing amounts of negatively charged protolytic form of dye with surface silanol and 3-aminopropyl groups (Figs. 4 and 10b). At the same time, MR-NH$_2$-MCM-41 demonstrates high selective sorption of MR from preferential majority of binary component solutions (Fig. 10b). In case of MR-NH$_2$-MCM-41, sorption process is affected by the above-mentioned hydrogen bonds along with $\pi-\pi$ stacking interactions arising between chemically immobilized MR-containing groups and dye moieties even in diluted solutions. It should be mentioned that removal of dyes from their binary component solutions in water attain greater values then in phosphate buffer. Perhaps, it is related with worse solubility and more pronounced aggregation of acid dyes used in sorption experiment in water medium.

3.   Conclusions

Our studies showed that selective sorption process may be optimized by control of the structural characteristics and protolytic state of silica surface as well as acid dye. Introduction of MR as structure directing agent in sol-gel synthesis has not influence on sorption properties of resulting MR$_{inc}$-NH$_2$-MCM-41 silica towards partially dissociated MR from single component system. At the same time, the noticeable suppression of sorption was observed for negatively charged dissociated MR and dyes with geometry similar or substantially different from MR. Sorptive removal of MR by NH$_2$-MCM-41 and MR$_{inc}$-NH$_2$-MCM-41 from all studied binary mixtures of dyes (except for ECB-containing one) is prevailing at pH 4.8 and proceeds less effectively at pH 5.5. Obviously, the key role in removal of MR by NH$_2$-MCM-41 and MR$_{inc}$-NH$_2$-MCM-41 from aqueous solutions belongs to the numerous hydrogen bonds, which become weaker at pH increasing from 4.8 to 5.5, and $\pi-\pi$ stacking interactions. Chemical immobilization of MR in silica surface layer causes drastic increase of sorptive removal of dyes from individual solutions and MR from binary solution due to $\pi-\pi$ stacking interactions arising between aromatic systems of chemically immobilized dye moieties and supplied from solution ones. The removal of MR is prevailing in preferential majority of studied aqueous mixtures. It can be concluded that the presence of MR suppresses sorption of another component of the mixture on synthesized organosilica materials.

So, silica sorbents with pronounced selectivity towards acid dye MR can be prepared by introduction of MR as part of the mixed micelles in sol-gel synthesis of organosilica materials as well as chemical immobilization of MR-containing groups in surface layer of organosilica. Obtained results could be useful in design of sorbents for selective dyes removal from effluents and optimization the separation process.

Appendix A. Supplementary data

Supplementary material associated with this article can be found, in the online version, at doi:10.1016/j.jes.2020.04.027.

REFERENCES

Abbas, F.S., 2013. Dyes removal from wastewater using agricultural waste. Adv. Environ. Biol. 1019–1026.

Abkenar, S.D., 2018. Fast and efficient removal of Acid Brown 214 from aqueous media by adsorption onto fluorene functionalized nanoporous SBA-15. Indian J. Chem. Technol. 25, 376–382.

Alaguprathana, M., Poonkothai, M., 2017. Decolourisation of the textile dye methyl red from aqueous solution using sugarcane bagasse pith. Asian J. Adv. Agric. Res. 37246, 1–9.

Anbia, M., Hariri, S.A., 2010. Removal of methylene blue from aqueous solution using nanoporous SBA-3. Desalination 261, 61–66.

Anbia, M., Hariri, S.A., Ashrafizadeh, S.N., 2010. Adsorptive removal of anionic dyes by modified nanoporous silica SBA-3. Appl. Surf. Sci. 256, 3228–3233.

Anbia, M., Salehi, S., 2012. Removal of acid dyes from aqueous media by adsorption onto amino-functionalized nanoporous silica SBA-3. Dyes Pigments 94, 1–9.

Barrett, E.P., Joyner, L.G., Halenda, P.H., 1951. The determination of pore volume and area distributions in porous substances. I. Computations from nitrogen isotherms. J. Am. Chem. Soc. 73, 373–380.

Belyakova, L.A., Besarab, L.N., Roik, N.V., Lyashenko, D.Yu., Vlasova, N.N., Golovkova, L.P., et al., 2006. Designing of the centers for adsorption of bile acids on a silica surface. J. Coll. Int. Sci. 294, 11–20.

Boukoussa, B., Hamacha, R., Morsli, A., Bengueddach, A., 2017. Adsorption of yellow dye on calcined or uncalcined Al-MCM-41 mesoporous materials. Arabian J. Chem. 10 (Supplement 2), S2160–S2169.

Bragg, W.L., 2013. The diffraction of short electromagnetic waves by a crystal. Proc. Camb. Philos. Soc. 17, 43–57.

Buvaneswari, N., Kannan, C., 2010. Adsorption of cationic and anionic organic dyes from aqueous solution using silica. J. Environ. Sci. Eng. 52 (4), 361–366.

Cho, Y.M., Lee, W.K., Kim, B.K., 1981. Studies on the interaction of azo dyes with cationic surfactant (I). Arch. Pharm. Res. 4 (2), 75–84.

Ebadi, A., Mohammadzadeh, J.S.S., Khudiev, A., 2009. What is correct form of BET isotherm for modeling liquid phase adsorption ? Adsorption 15, 65–73.

Enenebeaku, C.K., Okorocha, N.J., Uchechi, E.E., Ukaga, I.C., 2017. Adsorption and equilibrium studies on the removal of methyl red from aqueous solution using white potato peel powder. Int. Lett. Chem., Phys. and Astron. 72, 52–64.

Fenelonov, V.B., Romannikov, V.N., Derevyankin, A.Yu., 1999. Mesopore size and surface area calculations for hexagonal mesophases (types MCM-41, FSM-16, etc.) using low-angle XRD and adsorption data. Micropor. Mesopor. Mater. 28 (1), 57–72.

Foo, K.Y., Hameed, B.H., 2010. An overview of dye removal via activated carbon adsorption process. Desalin. Water. Treat. 19 (1–3), 255–274.

Freeman, H.S., Peter, A.T. (Eds.), 2000. Colorants for Non-Textile Applications. Elsevier Science, Amsterdam.

Ghaedi, M., Shokrollahi, A., Tavallali, H., Shojaiepoor, F., Keshavarz, B., Hossainian, et al., 2011. Activated carbon and multiwalled carbon nanotubes as efficient adsorbents for removal of arsenato(III) and methyl red from waste water. Toxicol. Environ. Chem. 93 (3), 438–449.

Ghemati, Dj., Aliouche, Dj, 2014. Dye adsorption behavior of polyvinyl alcohol/glutaraldehyde/β-cyclodextrin polymer membranes. J. Appl. Spec. 81 (2), 257–263.

Gehlen, M.H., Ferreira, M., Neumann, M.G., 1995. Interaction of methyl orange with cationic micelles and its effect on dye photochemistry. J. Photochem. Photobiol. A 87, 55–60.

Gregg, S.H., Sing, K.S., 1967. Adsorption, Surface Area and Porosity. Academic Press, New York.

Gritti, F., Guiochon, G., 2003. New thermodynamically consistent competitive adsorption isotherm in RPLC. J. Coll. Int. Sci. 264, 43–59.

Hamada, K., Kubota, H., Ichimura, A., Lijima, T., Amiya, S., 1985. Aggregation of an Azo dye in aqueous solution. Berichte Der Bunsengesellschaft Für Physikalische Chemie 89 (8), 859–863.

Hamada, K., Nonogaki, H., Fukushima, Y., Munkhbat, B., Mitsuishi, M., 1991. Effects of hydrating water molecules on the aggregation behavior of azo dyes in aqueous solutions. Dyes Pigments 16 (2), 111–118.

Ho, K.Y., Mckay, G., Yeung, K.L., 2003. Selective adsorbents from ordered mesoporous silica. Langmuir 19, 3019–3024.

Hosseinzadeh, R., Maleki, R., Matin, A.A., Nikkhahi, Y., 2008. Spectrophotometric study of anionic azo-dye light yellow (X6G) interaction with surfactants and its micellar solubilization in cationic surfactant micelles. Spectrochim. Acta A 69, 1183–1187.

Joo, J.B., Park, J., Yi, J., 2009. Preparation of polyelectrolyte-functionalized mesoporous silicas for the selective adsorption of anionic dye in an aqueous solution. J. Hazard. Mater. 168, 102–107.

Juang, L.C., Wang, C.C., Lee, C.K., 2006. Adsorption of basic dyes onto MCM-41. Chemosphere 64, 1920–1928.

Kang, J.K., Park, J.A., Kim, J.H., Lee, C.G., Kim, S.B., 2016. Surface functionalization of mesoporous silica MCM-41 with 3-aminopropyltrimethoxysilane for dye removal: kinetic, equilibrium, and thermodynamic studies. Desalin. Water Treat. 57 (15), 1–13.

Klaus, H. (Ed.), 2003. Industrial Dyes, Chemistry, Properties, Applications. Wiley-VCH, Weinheim.

Krysztafkiewicz, A., Binkowski, S., Jesionowski, T., 2002. Adsorption of dyes on a silica surface. Appl. Surf. Sci. 199, 31–39.

Lee, C.K., Liu, S.S., Juang, L.C., Wang, C.C., Lin, K.S., Lyu, M.D., 2007. Application of MCM-41 for dyes removal from wastewater. J. Hazard. Mater. 147, 997–1005.

Lewandowski, D., Olejnik, A., Schroeder, G., 2014. Adsorption studies and release of selected dyes from functionalized mesoporous MCM-41 silica. Cent. Eur. J. Chem. 12 (2), 233–241.

Mariani, G., Kutz, A., Di, Z., Schweins, R., Gröhn, F., 2017. Inducing hetero-aggregation of different azo dyes through electrostatic self-assembly. Chem. Eur. J. 23 (26), 6249–6254.

Mirzajani, R., Pourreza, N., Zayadi, A., Malakooti, R., Mahmoodi, H., 2016. Nanoporous calcined MCM-41 silica for adsorption and removal of Victoria blue dye from different natural water samples. Desalin. Water Treat. 57 (13), 5903–5913.

Nazar, M.F., Shah, S.S., Khosa, M.A., 2010. Interaction of azo dye with cationic surfactant under different pH conditions. J. Surfactants Deterg. 13 (4), 529–537.

Neimark, A.V., Ravikovitch, P.I., Grun, M., Schuth, F., Unger, K.K., 1998. Pore size analysis of MCM-41 type adsorbents by means of nitrogen and argon adsorption. J. Coll. Int. Sci. 207 (1), 159–169.

Neumann, B., Huber, K., Pollmann, P., 2000. A comparative experimental study of the aggregation of Acid Red 266 in aqueous solution by use of 19F-NMR, UV/Vis spectroscopy and static light scattering. Phys. Chem. Chem. Phys. 2 (16), 3687–3695.

Panic, V.V., Seslija, S.I., Nesic, A.R., Velickovic, S., 2013. Adsorption of azo dyes on polymer materials. Hem. Ind. 67 (6), 881–900.

Ratna Padhi, B.S., 2012. Pollution due to synthetic dyes toxicity and carcinogenicity studies and remediation. Int. J. Envir. Sci. 3 (3), 940–955.

Santhi, T., Manonmani, S., Smitha, T., 2010. Removal of methyl red from aqueous solution by activated carbon prepaped from the Anonna squmosa seed by adsorption. Chem. Eng. Res. Bull. 14 (1), 11–18.

Santhi, T., Manonmani, S., Smitha, T., Mahalakshmi, K., 2009. Adsorption kinetics of cationic dyes from aqueous solutions by bioadsorption onto activated carbon prepared from cucumis sativa. J. Appl. Sci. Env. Sanit. 4 (3), 263–272.

Santos, D.O., Santos, Md.L.N., Costa, J.A.S., de Jesus, R.A., Navickiene, S, Sussuchi, EM, et al., 2013. Investigating the potential of functionalized MCM-41 on adsorption of Remazol Red dye. Environ. Sci. Pollut. Res. 7, 5028–5035.

Saxena, R., Sharma, S., 2016. Adsorption and kinetic studies on the removal of methyl red from aqueous solutions using low-cost adsorbent: guargum powder. Int. J. Sci. Eng. Res. 7, 683–685.

Shah, M.P., 2018. Azo dye removal technologies. Austin J. Biotech. Bioeng. 5 (1), 1090–1096.

Singh, K., Arora, S., 2011. Removal of synthetic textile dyes from wastewaters: a critical review on present treatment technologies. Crit. Rev. Env. Sci. Tech. 41, 807–878.

Shariati-Rad, M., Irandoust, M., Amri, S., Feyzi, M., Ja'fari, F., 2014. Removal, preconcentration and determination of methyl red in water samples using silica coated magnetic nanoparticles. J. App. Res. Wat. Wast. 1, 6–12.

Singh, P.K., Singh, R.L., 2017. Bio-removal of azo dyes: a review. Int. J. Appl. Sci. Biotechnol. 5 (2), 108–126.

Tawarah, K.M., Khouri, S.J., 1992. The tautomeric and acid-base equilibria of p-methyl red in aqueous solutions. Dyes Pigments 20 (4), 261–270.

Tawarah, K.M., Wazwaz, A.A., 1993. The electrical conductivities of the sodium salts of methyl orange, o-methyl red and p-methyl red in aqueous solutions. Dyes Pigments 21 (2), 97–103.

Vital, R.K., Saibaba, K.V.N., Shaik, K.B., Gopinath, R., 2016. Dye removal by adsorption: a review. J. Bioremediat. Biodegrad. 7 (6), 371 (4 pages).

Weber, W.J., Morris, J.C., 1963. Kinetics of adsorption on carbon from solution. J. Sanit. Eng. Div. Am. Soc. Civ. Eng. 89, 31–60.

Wu, X., Hui, K.N., Hui, K.S., Lee, S.K., Zhou, W., Chen, R., et al., 2012. . Adsorption of basic yellow 87 from aqueous solution onto two different mesoporous adsorbents. Chem. Eng. J. 180, 91–98.

Wu, Y., Zhang, M., Zhao, H., Yang, S., Arkin, A., 2014. Functionalized mesoporous silica material and anionic dye adsorption: MCM-41 incorporated with amine groups for competitive adsorption of Acid Fuchsine and Acid Orange II. RSC Adv. 4, 61256–61267.

Zaharia, C., Suteu, D., 2012. Textile organic dyes – characteristics, polluting effects and separation/elimination procedures from industrial effluents. In: Puzyn, T., Mostrag-Szlichtyng, A. (Eds.), Organic Pollutants Ten Years After The Stockholm Convention - Environmental and Analytical Update. InTech, Croatia, pp. 55–87.

Zanjanchi, M.A., Sajjadi, H., Arvand, M., Mohammad-Khah, A., Ghalami-Choobar, B., 2011. Modification of MCM-41 with anionic surfactant: a convenient design for efficient removal of cationic dyes from wastewater. Clean Soil Air Water 39 (11), 1007–1013.

Zubieta, C., Sierra, M.B., Morini, M.A., Schulz, P.C., Albertengo, L., Rodriguez, M.S., 2008. The adsorption of dyes used in the textile industry on mesoporous materials. Colloid. Polym. Sci. 286, 377–384.